Intramolecular Interaction between Nitroxide Radical and Photoexcited Benzophenone Triplet Linked to Peptide Templates

ARTICLE *in* THE JOURNAL OF PHYSICAL CHEMISTRY A · AUGUST 2003

Impact Factor: 2.69 · DOI: 10.1021/jp0345203

8 AUTHORS, INCLUDING:

Elena Sartori
Ministero dell'Istruzione, dell'Università e del…
24 PUBLICATIONS **306** CITATIONS
SEE PROFILE

Simona Oancea
Lucian Blaga University of Sibiu
85 PUBLICATIONS **346** CITATIONS
SEE PROFILE

ARTICLES

Intramolecular Interaction between Nitroxide Radical and Photoexcited Benzophenone Triplet Linked to Peptide Templates

E. Sartori,[†] A. Toffoletti,[†] F. Rastrelli,[†] C. Corvaja,*[,†] A. Bettio,[‡] F. Formaggio,[‡] S. Oancea,[‡] and C. Toniolo[‡]

Department of Physical Chemistry and Institute of Biomolecular Chemistry, CNR and Department of Organic Chemistry, University of Padova, I-35131 Padova, Italy

Received: February 28, 2003; In Final Form: July 1, 2003

A series of heptapeptides and one dodecapeptide doubly labeled with a triplet precursor (4′-benzoylphenylalanine) and a nitroxide (4-amino-1-oxyl-2,2,6,6-tetramethylpiperidine-4-carboxylic acid) have been synthesized by solution methods and studied through their FT-IR absorption and time-resolved EPR spectra with UV laser pulse excitation. All of the oligopeptides show EPR nitroxide lines strongly polarized in emission because of the intramolecular interaction between the free radical and the photoexcited triplet. The kinetics of the time evolution of the EPR lines is analyzed to study the radical-triplet interaction in the series of heptapeptides characterized by diverging radical and triplet relative positions in the amino acid sequence.

Introduction

Quenching of excited triplets by free radicals and paramagnetic impurities was first reported many years ago.[1] This phenomenon was observed through its different effects (e.g., triplet lifetime shortening[2] and magnetic field dependence of photoconductivity).[3] In the early '90s, it was shown that in the presence of excited triplet species, the EPR lines of a free radical become polarized in emission or in enhanced absorption.[4] Anomalous line intensity is a consequence of the deviation of the spin level populations from the thermal equilibrium values. Such a polarization is caused by the spin selectivity of the triplet quenching process, which occurs through the formation of radical-triplet pairs (RTPs). As the RTPs produced in the doublet state by antiparallel coupling of the radical and triplet spin possess the same spin multiplicity of the pairs formed by ground-state singlet plus free radical, they decay fast, while RTPs in the quartet state, formed by parallel spin coupling, decay slowly. The radical-triplet pair mechanism (RTPM) of spin polarization is based on the selective mixing of doublet and quartet spin substates of the pair by electron spin dipolar and hyperfine interactions. These terms of the spin Hamiltonian do not commute with the Zeeman and exchange terms of the spin Hamiltonian of the pair.[4a] When the doublet and the quartet are separated by a nonvanishing exchange interaction, J, the extent of mixing depends on the z component of the electron spin total angular momentum. This fact produces spin polarization because the quartet components more contaminated with those of the doublet decay faster.

The existing RTPM theory is based on a model in which the quartet/doublet transitions are induced by the fluctuation of J during the relative diffusion of the RTP partners.[5] Indeed, J is expected to change exponentially with the radical-triplet distance.[6] The amount of polarization reaches a maximum when J is close to 1/3 and 2/3 of the Zeeman energy, because for these values, a crossing occurs between doublet and quartet spin sublevels. Even if efforts have been made to assess the relative distance between the partners in the pair, no clear-cut information is as yet available on this relationship. In addition to the knowledge of the exact dependence of J on the distance, other parameters should be considered, such as the correlation time for the diffusion process and the absolute value of the spin polarization, which is not easily obtained.[7] Moreover, it should be considered that a dependence of J exclusively on the radical-triplet distance is a reasonable assumption only for small molecules subjected to fast rotational diffusion. Under such conditions, any variation with the relative orientation of the partner is averaged out.

Recently, it has been shown that RTPM operates also when the radical and the triplet are covalently bound to the same molecule.[8] This observation suggested the possibility to investigate RTPs in which the partner distance range is well established. Moreover, by changing the spacer length, one could investigate the dependence of polarization intensity and kinetics on the radical-triplet distance.[9] A similar strategy was used in the study of spin-correlated radical pairs by producing two covalently linked free radicals by photoinduced Norrish I cleavage of cyclic ketones.[10]

In this paper, we present a time-resolved EPR (TR-EPR) study on a series of radical-triplet pairs, whose components are covalently linked at different relative positions on a rigid oligopeptide template. The radical is the nitroxide α-amino acid TOAC (4-amino-1-oxyl-2,2,6,6-tetramethylpiperidine-4-carboxylic acid) (Figure 1),[11] while the triplet excited species is the benzophenone moiety of L-Bpa (4′-benzoylphenylalanine)

* To whom correspondence should be addressed. E-mail: carlo.corvaja@unipd.it.
[†] Department of Physical Chemistry.
[‡] Department of Organic Chemistry.

10.1021/jp0345203 CCC: $25.00
Published on Web 08/16/2003

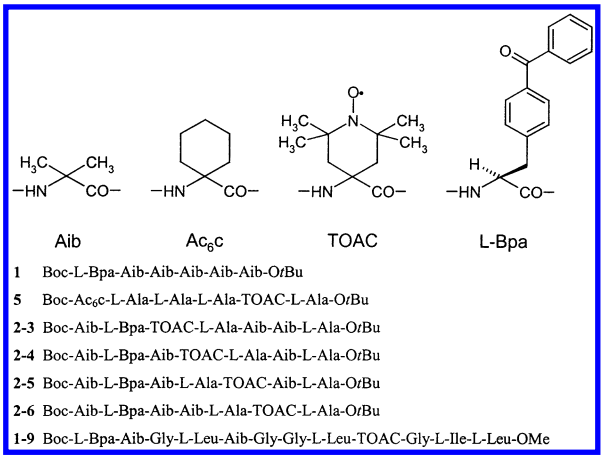

Figure 1. Chemical structures of amino acids and sequences of peptides investigated in this work.

(Figure 1).[12] A preliminary account on the TR-EPR technique applied to peptide systems has already been reported.[8e] The present study pointed at determining a TR-EPR parameter sensitive to the radical-triplet distance. To this aim, we synthesized four 3_{10}-helical[13] model heptapeptides (**2**−**3**, **2**−**4**, **2**−**5**, and **2**−**6**) in which the triplet moiety (L-Bpa) is kept at position 2, while the radical group (TOAC) is moved along the peptide chain toward the C-terminus from position 3 to position 6 (Figure 1). Thus, the radical-triplet separation in the sequence covers more than one turn of the ternary helix. In addition, we added the L-Bpa residue at the N-terminus of the (TOAC[8]−L-Leu[11]−OMe) trichogin GA IV[14] analogue (peptide **1**−**9**) (Figure 1) to insert more than two helix turns between the radical and the triplet. All peptide molecules used as templates in this work possess a rigid, helical backbone structure because of their high content in C^{α}-tetrasubstituted α-amino acids, known to be strong promoters of helical conformations.[15] This feature allows a reliable prediction of intramolecular distances. However, while the nitroxide side-chain moiety of TOAC is tightly connected to the peptide backbone through a rigid six-membered ring, the side-chain benzophenone group of L-Bpa experiences a significant conformational freedom owing to the allowed rotations around the two σ bonds ($C^{\alpha}-C^{\beta}$ and $C^{\beta}-C^{\gamma}$ bonds) which link it to the peptide main chain. Therefore, in calculating the distance between the radical-triplet pair studied here, one has to take into account the possible fluctuation of the benzophenone moiety. Despite this, we chose for the present study the benzophenone-containing, L-Bpa residue for the following reasons: (i) Benzophenone is the most extensively used triplet precursor system in RTPM studies because of its high triplet yield and its fully understood photophysical and magnetic properties; (ii) L-Bpa has been already exploited in peptide and protein investigations because of its ability to promote cross-linking by photoactivation;[12] and (iii) L-Bpa is commercially available and can be incorporated into a peptide chain as a standard protein amino acid.

Experimental Section

Synthesis and Characterization. TOAC was synthesized according to published procedures.[11,16] The L-Bpa/TOAC heptapeptides studied in this work (**2**−**3**, **2**−**4**, **2**−**5,** and **2**−**6**) (Figure 1) were prepared manually in a 20−30 mg scale by the step-by-step strategy in solution, beginning from the C-terminal residue. As TOAC is unstable under the acidic and reducing conditions required to remove the classical Boc (*tert*-butyloxycarbonyl) and Z (benzyloxycarbonyl) groups, the Fmoc (9-fluorenylmethyloxycarbonyl) N^{α}-protecting group was chosen for the elongation of the peptide chain. The Fmoc group was removed by treatment with a 20% v/v diethylamine solution in CH_2Cl_2. Given the low reactivity of C^{α}-tetrasubstituted α-amino acids in peptide bond formation, the highly efficient EDC/HOAt [EDC, 1-(3-dimethylaminopropyl)-3-ethylcarbodiimide; HOAt, 1-hydroxy-7-aza-1,2,3-benzotriazole][17] condensation method was used in coupling reactions involving Aib (α-aminoisobutyric acid), Ac_6c (1-aminocyclohexane-1-carboxylic acid), or TOAC. The L-Bpa-containing trichogin GA IV analogue **1**−**9** (Figure 1) was prepared by condensing the commercially available Boc−L-Bpa−OH with the free amine of (TOAC[8], -Leu[11]−OMe (OMe, methoxy))trichogin GA IV (obtained by N-deprotection of the corresponding Fmoc undecapeptide[14c]). Peptide **1** (Figure 1), incorporating the triplet precursor Bpa (at position 1) only, was synthesized by condensing Boc−L-Bpa−OH with H−$(Aib)_5$−O*t*Bu (O*t*Bu, *tert*-butoxy) (obtained by N-deprotection of Z−$(Aib)_5$−O*t*Bu[18] via catalytic hydrogenolysis). Peptide **5** (Figure 1), bearing the nitroxide label (at position 5) only, was prepared from Boc−Ac_6c−OH and H−L-Ala−L-Ala−L-Ala−TOAC−L-Ala−O*t*Bu (the latter obtained, in turn, from the corresponding Fmoc-protected pentapeptide[19]). A column chromatography purification was required after each coupling step. More specifically, for the final L-Bpa/TOAC heptapeptides, we used a flash chromatography purification on a silica gel column (ICN Biomedicals), 32−63-μm mesh, with a gradient elution either from 0 to 5% ethanol in chloroform or from 33 to 100% ethyl acetate in petroleum ether. Finally, the derivative Boc−L−Met−OMe (Met, methionine) was prepared by acylating the commercially available HCl·H−L−Met−OMe with $(Boc)_2O$.[20]

All peptides were characterized by melting point and optical rotatory power determinations, thin-layer chromatography (TLC) in three solvent systems, and solid-state IR absorption (Table 1).

Sample Preparation and EPR Measurements. The 1-mM and 5-mM peptide solutions in acetonitrile (Fluka, ≥ 99.5 (GC)) were prepared without any further purification of the solvent. The solutions, transferred in quartz tubes (1 mm inner diameter), were then degassed by repeated pump-freeze-thaw cycles and sealed under vacuum. The experimental setup used for TR-EPR measurements comprises a conventional X-band EPR spectrometer (Bruker ER 200 D) equipped with temperature control accessories and an excimer laser (Lambda Physik LPX 100, XeCl, λ = 308 nm, pulse width = 20 ns). A few experiments were performed using the third harmonic (λ = 355 nm) of a Nd/YAG solid-state laser (Brilliant Quantel). The EPR transient signals, generated by the laser pulses, were recorded without field modulation, with a preamplifier (bandwidth: 20 Hz−6.5 MHz) and a digital oscilloscope (LeCroy 9450A) that averages them. 2D-TR-EPR spectra were obtained by transferring the averaged transients acquired at each field address to a PC, where they were treated with a homemade software. To correct the data for the cavity response to the laser perturbation, an off-resonance signal was subtracted from the transient signals recorded at all of the field positions of the 2D-TR-EPR surface.

Conformational Energy Calculations. Conformational energies were obtained by performing molecular mechanics calculations with HyperChem (release 6.02).[21] The MM^{+} force field was employed.

Results and Discussion

Conformational Analysis. The paramagnetic character of the TOAC nitroxide prevents the use of the ^{1}H NMR technique for

TABLE 1: Physical Properties for the TOAC and/or L-Bpa-Containing, Newly Synthesized Peptides

peptide[a]	yield[b] (%)	melting point (deg C)	crystalliz. solvent[c]	$[\alpha]_D^{20}$ (deg)[d]	TLC[f] R_{F1}	R_{F2}	R_{F3}	IR (cm^{-1})[g]
Fmoc−TOAC−Aib−L-Ala−O*t*Bu	51	182−184	$CHCl_3$−PE	−33.1[e]	0.90	0.95	0.40	3350, 3278, 1717, 1666, 1529
Fmoc−TOAC−L-Ala−Aib−L-Ala−O*t*Bu	52	108−110	EtOAc−PE	−18.0	0.80	0.95	0.35	3340, 1705, 1663, 1529
Fmoc−L-Ala−TOAC−Aib−L-Ala−O*t*Bu	69	118−120	$CHCl_3$−PE	−66.8	0.85	0.95	0.40	3346, 1726, 1684, 1526
Fmoc−Aib−L-Ala−TOAC−L-Ala−O*t*Bu	71	94−95	$CHCl_3$−PE	−38.5	0.75	0.95	0.35	3333, 1730, 1703, 1668, 1528
Fmoc−Aib−Aib−L-Ala−TOAC−L-Ala−O*t*Bu	40	107−109	$CHCl_3$−PE	−13.1	0.75	0.95	0.30	3325, 1729, 1664, 1529
Fmoc−Aib−L-Ala−TOAC−Aib−L-Ala−O*t*Bu	60	110−112	$CHCl_3$−PE	−47.4	0.80	0.95	0.35	3334, 1726, 1662, 1526
Fmoc−Aib−TOAC−L-Ala−Aib−L-Ala−O*t*Bu	51	129−130	$CHCl_3$−PE	+3.8	0.95	0.95	0.35	3338, 1728, 1668, 1528
Fmoc−TOAC−L-Ala−Aib−Aib−L-Ala−O*t*Bu	82	108−110	$CHCl_3$−PE	−24.8	0.65	0.90	0.30	3330, 1704, 1662, 1528
Fmoc−L-Bpa−Aib−Aib−L-Ala−TOAC−L-Ala−O*t*Bu	48	121−123	$CHCl_3$−PE	−27.3	0.75	0.95	0.35	3327, 1724, 1662, 1529
Fmoc−L-Bpa−Aib−L-Ala−TOAC−Aib−L-Ala−O*t*Bu	56	126−128	$CHCl_3$−PE	−29.0	0.90	0.95	0.35	3328, 1723, 1660, 1527
Fmoc−L-Bpa−Aib−TOAC−L-Ala−Aib−L-Ala−O*t*Bu	55	132−134	$CHCl_3$−PE	+34.9	0.80	0.95	0.35	3336, 1728, 1660, 1530
Fmoc−L-Bpa−TOAC−L-Ala−Aib−Aib−L-Ala−O*t*Bu	60	140−142	$CHCl_3$−PE	−24.8	0.65	0.95	0.35	3334, 1727, 1660, 1529
Boc−L-Bpa−Aib−Aib−Aib−Aib−Aib−O*t*Bu	80	136−138	EtOAc−PE	−9.6[e]	0.70	0.95	0.40	3327, 1731, 1663, 1529
Boc−Ac_6c−L-Ala−L-Ala−L-Ala−TOAC−L-Ala−O*t*Bu	66	138−140	$CHCl_3$−PE	−16.2	0.80	0.95	0.45	3310, 1734, 1695, 1662,1529
Boc−Aib−L-Bpa−Aib−Aib−L-Ala−TOAC−L-Ala−O*t*Bu	55	107−109	$CHCl_3$−PE	−28.0[e]	0.75	0.95	0.25	3318, 1730, 1662, 1529
Boc−Aib−L-Bpa−Aib−L-Ala−TOAC−Aib−L-Ala−O*t*Bu	63	115−117	$CHCl_3$−PE	−22.4	0.90	0.95	0.30	3323, 1728, 1660, 1530
Boc−Aib−L-Bpa−Aib−TOAC−L-Ala−Aib−L-Ala−O*t*Bu	52	115−117	$CHCl_3$−PE	−22.7	0.80	0.95	0.30	3334, 1729, 1659, 1531
Boc−Aib−L-Bpa−TOAC−L-Ala−Aib−Aib−L-Ala−O*t*Bu	63	110−112	$CHCl_3$−PE	−26.4	0.65	0.95	0.20	3326, 1728, 1660, 1528
Boc−L-Bpa−Aib−Gly−L-Leu−Aib−Gly−Gly−L-Leu−TOAC−Gly−L-Ile−L-Leu−OMe	67	170−171	CH_3CN-H_2O	−9.2	0.25	0.80	0.05	3333, 1738, 1656, 1534

[a] All chiral residues are of L (S)-configuration. [b] The yield refers to the final coupling step. [c] EtOAc = ethyl acetate; PE = petroleum ether (60−80 °C). [d] $c = 0.25$, MeOH. [e] $c = 0.50$, MeOH. [f] Thin-layer chromatography was performed on Merck Kiesegel $60F_{254}$ precoated plates using the following solvent systems: I ($CHCl_3$/EtOH, 9:1), II (1-BuOH/HOAc/H_2O, 3:1:1), III (toluene/EtOH, 7:1). [g] The IR absorption spectra were obtained in KBr pellets; only bands in the 3500−3200 and 1800−1500 cm^{-1} regions are shown.

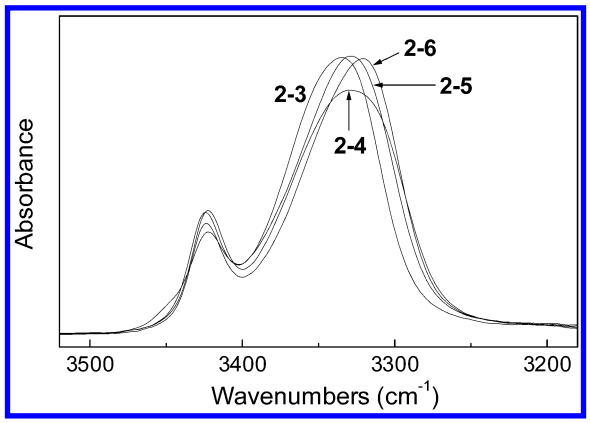

Figure 2. FT-IR absorption spectra in the amide A (N−H stretching) region of peptides **2**−**3**, **2**−**4**, **2**−**5**, and **2**−**6** in $CDCl_3$ solution (1 mM).

a conformational study of our peptides. Little information can be extracted also from circular dichroism measurements, because spectra interpretation is hampered by TOAC[22] and Bpa electronic absorptions in the conformationally informative far-UV region (250−190 nm). Therefore, the structural preferences of heptapeptides **2**−**3**, **2**−**4**, **2**−**5** and **2**−**6** were investigated by means of FT-IR absorption spectroscopy in $CDCl_3$ solution at three peptide concentrations. H-Bond acceptor solvents, such as acetonitrile, are less useful, as it is difficult to discriminate between N−H···solvent and N−H···O═C H-bonds in the usually informative amide A (N−H stretching) region (3500−3200 cm^{-1}).

The FT-IR absorption spectra in $CDCl_3$ solution at 1 mM peptide concentration for the four heptapeptides are illustrated in Figure 2. Relevant conclusions are the following: (i) The weak band centered at about 3425 cm^{-1} is assigned to free, solvated peptide NH groups, while the intense band at about 3330 cm^{-1} is assigned to H-bonded peptide NH groups.[23] (ii) The spectra do not change appreciably in the concentration range examined (10−0.1 mM) (spectra not shown), thus indicating that the 3330 cm^{-1} band is due essentially to intramolecularly H-bonded peptide NH groups. (iii) The high values of the A_H/A_F ratio (integrated intensity of the band of H-bonded NH groups to free NH groups)[23,24] are indicative of a stable helical secondary structure. In addition, in all peptides, the position of the absorption maximum for the amide I (C═O stretching) band (data not shown) is close to the values typical of α- and 3_{10}-helices.[25] Taken together, these observations indicate that the peptides studied in this work largely adopt intramolecularly H-bonded helical structures in $CDCl_3$ solution. In view of their short main-chain length, it is plausible that the type of helix adopted by heptapeptides **2**−**3**, **2**−**4**, **2**−**5,** and **2**−**6** would be the 3_{10}-helix.[15] Peptide **1**−**9**, a trichogin GA IV analogue, is expected to fold in a mixed α-/3_{10}-helical conformation as its parent peptide[14,26] and a number of TOAC-containing analogues.[27]

TR-EPR Measurements. Upon UV photoexcitation, all four heptapeptides give TR-EPR spectra consisting of three lines in emission, placed at the magnetic field positions expected for the three hyperfine components of the nitroxide radical (g = 2.0061, a_N = 1.5 mT). Their decay times are of the order of a few microseconds. The signal intensity does not change appreciably in the series **2**−**3**, **2**−**4**, **2**−**5,** and **2**−**6**, while a less intense signal is observed for **1**−**9**. However, a small but significant variation is observed in the kinetic parameters within the series (Table 2).

Figures 3(a) and 4(a) show the 2D-TR-EPR signals of peptides **2**−**5** and **1**−**9**, respectively, displayed as a function of magnetic field and time, while Figures 3(b) and 4(b) show the signal time evolutions of the three hyperfine components. To establish whether the observed spin polarization of the nitroxide EPR lines is due to an intramolecular or an intermolecular triplet quenching process, a series of measurements was carried out for peptide samples at two different concentrations, namely 5 mM and 1 mM. Moreover, TR-EPR spectra were recorded also for solutions of peptide **5** (labeled only with TOAC) in the presence of either benzophenone or peptide **1** (labeled only with L-Bpa). Because of the UV irradiation (λ = 308 nm) all samples undergo a degradation process that produces a decrease of the TR-EPR signal intensity. However, this process is slow enough to allow recording of complete 2D-TR-EPR spectra of the samples. The results are discussed below.

TABLE 2: Kinetic Parameters Employed to Fit the Nitroxide Time Evolution for the Different Peptides with $k_2 = 1/T_1$ and $k_3 = 1/\tau + k_q$

		low-field line		central line		high-field line	
peptide	conc (mM)	k_2 (10^6 s^{-1})	k_3 (10^6 s^{-1})	k_2 (10^6 s^{-1})	k_3 (10^6 s^{-1})	k_2 (10^6 s^{-1})	k_3 (10^6 s^{-1})
2−3	1	3.84	0.59	2.94	**0.52**	3.57	0.46
	5	3.13	0.56	2.94	**0.58**	2.86	0.54
2−4	1	2.33	0.62	3.57	**0.47**	*a*	*a*
	5	2.94	0.70	3.57	**0.65**	3.33	0.58
2−5	1	2.94	0.61	2.50	**0.59**	2.38	0.56
	5	3.45	0.63	3.03	**0.63**	3.33	0.59
2−6	1	3.23	0.58	2.86	**0.56**	3.70	0.48
	5	2.63	0.64	2.50	**0.63**	2.56	0.57
1−9	1	3.23	0.59	2.86	**0.51**	3.57	0.40
	5	3.03	0.60	2.94	**0.57**	3.03	0.48
5 + B[b]	1	*a*	*a*	*a*	*a*	*a*	*a*
	5	4.76	0.70	4.76	**0.56**	4.55	0.62
5 + 1	1	1.67	0.50	2.00	**0.34**	2.38	0.20
	5	3.03	0.75	2.63	**0.72**	2.40	0.71

[a] Value not measurable because of a poor signal-to-noise ratio. [b] **B**, benzophenone.

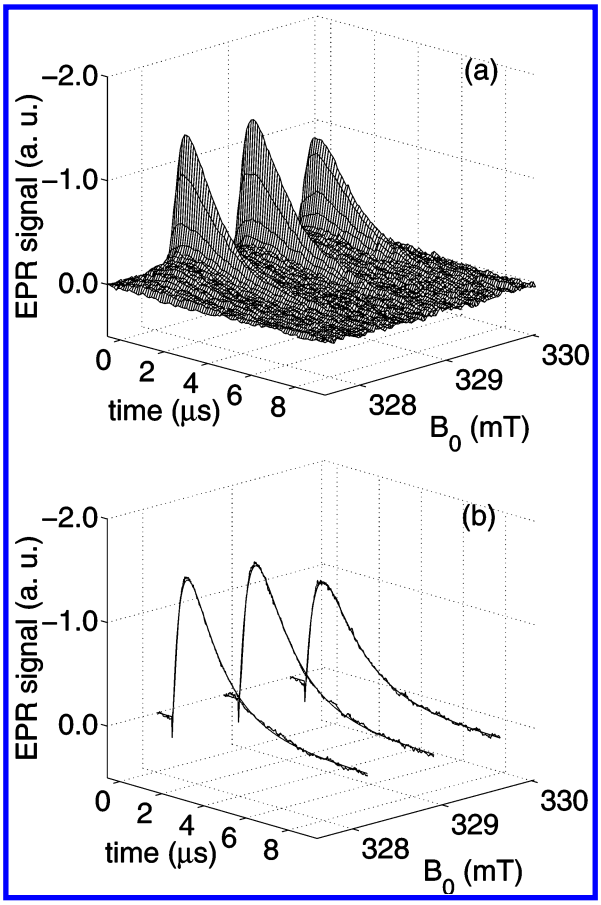

Figure 3. (a) 2D-TR-EPR spectrum of peptide **2−5** (1 mM in acetonitrile), 280 K, 12 dB; (b) sections of the 2D-TR-EPR spectrum taken at the field positions corresponding to the three hyperfine lines and their fit.

Kinetics of Triplet Quenching by Free Radicals. Let us consider the radical-triplet quenching reaction:

$$R + {}^3B \rightleftarrows [R\ {}^3B] \rightarrow R^* + B$$

in which R is the nitroxide group of the TOAC residue, ^{3}B is the triplet excited benzophenone chromophore of the Bpa residue and R* represents the spin polarized radical. In the case of separated species [R ^{3}B] is a transient RTP complex, formed in

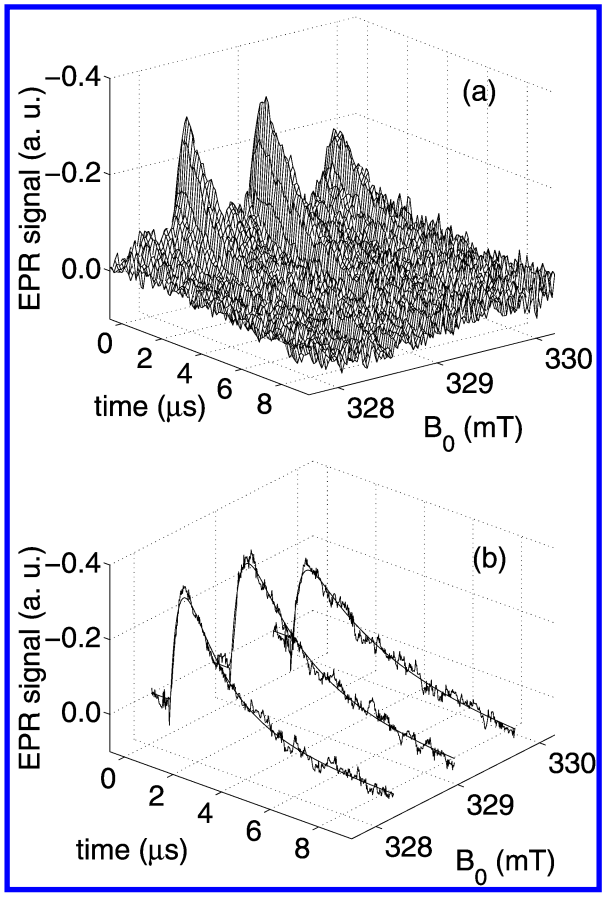

Figure 4. (a) 2D-TR-EPR spectrum of peptide **1−9** (1 mM in acetonitrile), 280 K, 12 dB; (b) sections of the 2D-TR-EPR spectrum taken at the field positions corresponding to the three hyperfine lines and their fit.

solution during the nitroxide triplet benzophenone encounters, which are, in turn, related to the relative diffusion of the two partner molecules. However, for systems in which the two partners are covalently linked to the same molecule, formation of RTP does not need diffusion. In that case, [R ^{3}B] is representative of a specific conformation of the molecule, suitable for triplet quenching interaction.

The TR-EPR signal of R is proportional to the y component of the magnetization, M_y, in a reference frame rotating around the Zeeman magnetic field direction, indicated by z. Then, x is the direction of the microwave field B_1, assumed to oscillate at the Larmor frequency ω_0. M_y is obtained by solving the relevant Bloch equations, modified by taking into account kinetic terms deriving from the radical-triplet interaction, and a third equation for the time-dependent triplet concentration $[^3B](t)$.[28] They are:

$$\frac{dM_y(t)}{dt} = -M_y(t)\frac{1}{T_2} + M_z(t)\omega_1 \quad (1.1)$$

$$\frac{dM_z(t)}{dt} = -M_y(t)\omega_1 + (P_{eq}^R[R] - M_z(t))\frac{1}{T_1} + P_{RTPM}^R k_q[^3B](t) \quad (1.2)$$

$$\frac{d[^3B](t)}{dt} = -[^3B](t)\left(\frac{1}{\tau} + k_q\right) \quad (1.3)$$

In equation 1, τ represents the benzophenone triplet lifetime in the absence of radical quenching, k_q is the quenching rate

constant, and P^R_{eq} and P^R_{RTPM} are the radical polarization factors. P^R_{eq} refers to the thermal equilibrium in the absence of microwaves and P^R_{RTPM} to the RTPM polarization. T_1 and T_2 are the radical relaxation times, and $\omega_1 = \gamma B_1$, $M_y(t)$, and $M_z(t)$ have their usual meaning.

The analytical solution for $M_y(t)$ obtained from these equations consists of a sum of three exponential functions of t, the rate constants of which are simple functions of the relaxation times T_1 and T_2, the Rabi frequency ω_1, the triplet lifetime τ, and the triplet quenching rate constant k_q.

$$M_y(t) = A + Be^{-k_1 t} + Ce^{-k_2 t} + De^{-k_3 t} \tag{2.1}$$

$$k_1 = \frac{(T_1 + T_2 + \sqrt{(T_1 + T_2)^2 - 4T_1T_2(1 + T_1T_2\omega_1^2)})}{2T_1T_2} \tag{2.2}$$

$$k_2 = \frac{(T_1 + T_2 - \sqrt{(T_1 + T_2)^2 - 4T_1T_2(1 + T_1T_2\omega_1^2)})}{2T_1T_2} \tag{2.3}$$

$$k_3 = \left(\frac{1}{\tau} + k_q\right) \tag{2.4}$$

Because of the zero preamplifier gain at low frequency (cut off at $\nu < 20$ Hz), the constant term A, which represents the equilibrium magnetization in the presence of microwaves, is not recorded in the TR-EPR spectra.[7] The corresponding expressions for the preexponential factors B, C, and D ($B + C + D = 0$), are more complicated. They depend on the same parameters that appear in eqs (2.2)−(2.4), on the initial conditions ($M_y(0)$, $M_z(0)$, $[^3B](0)$), and on the polarization parameters P^R_{eq} and P^R_{RTPM} (which cannot be determined if A is not measured).

Equations 2.2 and 2.3 show that for low microwave power ($T_1T_2\omega_1^2 \ll 1$), the rates k_1 and k_2 reduce to $k_1 = -1/T_2$ and to $k_2 = -1/T_1$. Moreover, the kinetic information about the quenching rate is contained in k_3. For nitroxide radicals in low viscosity liquids, $T_1 \approx T_2$. Indeed, T_1 values in the range 200−600 ns and T_2 values of 380 ns have been measured at the same temperature of our experiments.[29] Therefore, the time evolution of the EPR signal will be well approximated by the sum of two exponential functions with rate constants k_2 and k_3 convoluted with the instrument response function.[30] It should be noted that, using the largest values found in the literature for T_1 and T_2, k_1 and k_2 are still dominated by the relaxation times as long as $\omega_1 \leq 2.1 \times 10^6$ s^{-1}. Under our experimental conditions, the value of ω_1 is estimated to be 0.53×10^6 s^{-1}.

The foregoing kinetic treatment is valid for both inter- and intramolecular quenching processes, the only difference being the meaning of the constant k_q. For intermolecular quenching, k_q should be considered as a pseudo-first-order rate constant proportional to the radical concentration (i.e., $k_q = k[R]$), while for intramolecular quenching, k_q is a first-order rate constant not dependent on [R].

Intramolecular Triplet Quenching in the Peptides Series. In our peptide systems, the benzophenone triplet quenching by the nitroxide radical could in principle be either an intermolecular or an intramolecular process, as already found in other doubly labeled peptides.[8e,31]

The two types of contribution are discussed in this section.

The TR-EPR signals recorded for solutions of peptide **5** (1 mM) and benzophenone (1 mM) or of peptide **5** (1 mM) and peptide **1** (1 mM) are remarkably less intense than those recorded for 1 mM solutions of peptides **2**−**3**, **2**−**4**, **2**−**5**, **2**−**6**, and even **1**−**9**, where the triplet moiety (L-Bpa) and the radical (TOAC) are covalently linked to the same molecule. In particular, for the solution of peptide **5** and benzophenone, the signal is barely observable over the noise (S/N ≈ 2), while for the doubly labeled peptides, the signal-to-noise ratio depends on the particular peptide and varies from 6 for **1**−**9** to 24 for **2**−**5**. Moreover, when the triplet chromophore and the radical are not both bound to the same peptide, as in the mixture of peptides **1** and **5**, we observed that the sample degradation due to the UV irradiation occurs much faster.

Within our series of doubly labeled peptides the strongest signal is obtained for peptide **2**−**5** and the weakest for peptide **1**−**9**. We note that the amino acid side chains of residues 2 and 5 in the peptide chain are one on top of the other after a complete turn of the ternary helix, so that the triplet and the radical are facing each other in a favorable position for interacting, while in peptide **1**−**9** they are separated by more than two helix turns.

It would be tempting to correlate the signal intensity with the distance between the labels. This would be justified if the signal intensity were dependent on the quenching efficiency. However, our experimental conditions do not allow the relative signal intensity of two samples to be precisely determined, because the measurements of each peptide sample required changing the sample tube in the EPR cavity and modifying the instrumental conditions. Unfortunately, the use of a cell in which the solution could flow [4a,b] was prevented by the small quantities of labeled peptides in our hands.

Because of these drawbacks, we examined the possibility to rely on the kinetic parameters, and particularly on k_3.

From Table 2, we note that the rate constant k_3 is different for the different hyperfine components, whereas eq 2.4 predicts the same value. This effect has to be attributed to the Heisenberg spin exchange process. In the comparison of the kinetic parameters of the different peptides, we used the fitting of the central line (entries in bold in Table 2), which is not affected by the exchange.[32] The rate of this process is too low to affect the EPR line width, but it does influence the kinetics of the different hyperfine components.[8e] Indeed, we observed the expected spin exchange transfer polarization from the low-field line to the high-field line, the decay of the former becoming faster and that of the latter becoming slower.

Even T_1 is not the same for the different hyperfine components, but this finding is not surprising, because different spin−lattice relaxation times have been indeed measured for the different hyperfine components of nitroxide radicals.[28]

The rate constant k_3 would be almost equal to k_q (eq 2.4) if the triplet lifetime τ in our solutions could be assumed to be equal to that reported in the literature for benzophenone triplet in the same solvent (50 μs).[33] In this case, the contribution $1/\tau$ would be quite small ($\sim 0.02 \times 10^6$ s^{-1}) in comparison to the best fit values of k_3, which are in the range $0.40-0.70 \times 10^6$ s^{-1}.

If the quenching process were intermolecular *and* diffusion controlled, as found by several authors[4b,5b,34] when benzophenone is photoexcited in a solution containing TEMPO radicals, the rate constant k of the bimolecular reaction at $T = 280$ K, taking into account the solvent (acetonitrile) viscosity,[35] is expected to be 1.65×10^{10} M^{-1} s^{-1}. Consequently, at 1 mM peptide concentration, the diffusion controlled pseudo-first-order rate constant k_q should be 16.5×10^6 s^{-1} and 82.5×10^6 s^{-1} for a 5 mM solution. We note that the latter values are much larger than those found in our experiments (Table 2). Thus, the quenching process cannot be completely accounted for by an intermolecular *and* diffusion controlled process.

Nevertheless, we found different k_3 values for 1 mM and 5 mM peptide solutions. However, a 5-fold increase in the concentration does not result in a corresponding increase of k_3. If one considers the observed variation on increasing the concentration as due to an intermolecular contribution, the latter would be accounted for by a bimolecular rate constant k in the range $1-2 \times 10^7$ M^{-1} s^{-1}. A TR-EPR investigation was also performed on a solution of peptide **5** (5 mM), which does not contain Bpa, and benzophenone (5 mM). For this system, in which only an intermolecular quenching is possible, k_3 was found to be of the same order of magnitude as that of the doubly labeled peptides.[36] We conclude that even in this case, the reaction rate is not diffusion controlled, indicating that a significant number of molecular collisions is not effective in triplet quenching.

For the double labeled peptides, taking into account the intermolecular contribution and still neglecting the term $1/\tau$, the intramolecular contribution to k_3, k_{intra}, turns out to be 0.50×10^6 s^{-1} for **2−3**, 0.45×10^6 s^{-1} for **2−4**, 0.58×10^6 s^{-1} for **2−5**, 0.54×10^6 s^{-1} for **2−6**, and 0.49×10^6 s^{-1} for **1−9**.

The most relevant conclusion is that for all heptapeptides in the series, and even for peptide **1−9**, a spin polarization due to intramolecular triplet quenching is observed. This finding strongly suggests that for all systems investigated here there is a favorable conformation in which the two partners are close enough to interact.

The rate constant k_{intra} increases in the order **2−4** < **1−9** < **2−3** < **2−6** < **2−5**. These rate constants are amazingly similar despite the differing geometries. However, their differences are larger than the experimental error (estimated to be 0.01×10^6 s^{-1}).

There could be two explanations for this fact: either the flexibility of the L-Bpa peptide link does not allow differentiation of the L-Bpa−TOAC distance or the radical-triplet interaction is only weakly distance dependent.

The similarity of the k_{intra} values could suggest that the contribution of the triplet lifetime ($1/\tau$) to k_3 is not negligible.

In any case, these results are in line with EPR measurements performed on a series of analogous 3_{10}-helix forming peptides doubly labeled with TOAC.[19] For those peptides, the trend of the radical−radical exchange interaction (J value), inferred from the CW-EPR measurements, is 1−3 < 1−5 < 1−4 < 1−2, showing that also in that case, the interaction has the smallest value when the two probes residues are separated by one amino acid residue. That trend, in which the strongest interaction is exhibited by the peptide in which the labels are contiguous, was justified assuming that both a through-space and a through-bond mechanism were operative. In our case, the through-space mechanism seems to be dominant in the radical-triplet pair interaction.

Simple molecular mechanics calculations were performed in order to derive the radical-triplet distances and to test the consistency of these results. For the peptide backbone a rigid structure was assumed, based on the characteristic torsion angles of the right-handed 3_{10}-helical structure[13] ($\phi = -57°$; $\psi = -30°$), while the benzophenone group of L-Bpa was allowed to rotate around the two single bonds ($C^\alpha-C^\beta$ and $C^\beta-C^\gamma$ bonds) connecting it to the peptide backbone. Even if such calculations are quite crude, we nevertheless believe that they can be exploited for a qualitative discussion of our results.

The $-C^\beta H_2-$benzophenone potential energy was calculated (by single point calculations) and displayed in a two-dimensional plot as a function of the two torsion angles, which describe the rotations around the two single bonds mentioned above. For all peptides, some potential energy minima can be located, and in most of the cases (except for **2−3**), they are observed to occur when the torsion angle about the $C^\alpha-C^\beta$ is about 60, 180, and 300° and the torsion angle about the $C^\beta-C^\gamma$ is about 90 and 270°, as listed in detail in Table 3. Only some of these minimum energy conformations, expected to be significantly populated, were used for radical-chromophore distance evaluation.[37] For each of the significantly populated conformations we calculated the distances between all the chromophore π-system atoms and the nitrogen atom of TOAC. The shortest distance for each conformation, $d(RT)_{min}$, is reported in Table 3. In peptide **2−4** the TOAC-benzophenone shortest distance (in this case from nitrogen of TOAC to C^γ of L-Bpa) $d(RT)_{min} = \sim 9.6$ Å and it does not change upon changing the conformation. Despite the large number of residues separating the two partners, in each accessible conformation of peptide **1−9** there are chromophore π atoms rather close to the nitroxide group, $d(RT)_{min}$ being in the range 7.0−7.5 Å. Peptides **2−3**, **2−5**, and **2−6** show $d(RT)_{min}$ in the ranges 5.5−7.3, 6.2−8.8, and 5.0−8.7 Å, respectively. They differ from peptide **2−4** in the shortest allowed distance, which is smaller for **2−3**, **2−5**, and **2−6** and in the amplitude of the variation range. Qualitatively, these theoretical results are in agreement with the experimental rank order for the rate constants. The shortest distances, $d(RT)_{min}$, for the accessible conformations are listed in Table 3.

TABLE 3: Torsion Angles, Energies of $-C^\beta H_2$-Benzophenone, and Shortest Radical-Triplet Distances of the Minimum Energy Conformations Considered Accessible[a]

peptide	torsion angles[b] about $C^\alpha-C^\beta$ and $C^\beta-C^\gamma$ (deg)	energy (kcal mol^{-1})	$d(RT)_{min}$[c] (Å)
2−3	(170, 70)	79.2	5.6
	(170, 250)	79.7	5.5
	(330, 280)	80.1	6.9
	(340, 120)	80.1	6.7
	(320, 140)	80.2	7.3
2−4	(60, 270)	19.2	9.6
	(60,90)	20.6	9.6
2−5	(50, 280)	20.9	8.8
	(70, 110)	21.9	8.6
	(50, 90)	21.9	8.8
	(180, 80)	22.6	6.3
	(180, 260)	22.9	6.2
2−6	(60, 280)	20.3	8.4
	(80, 110)	20.7	8.0
	(160, 80)	21.4	5.0
	(170, 70)	21.4	5.5
	(50, 90)	21.5	8.7
	(160, 250)	22.6	6.1
1−9	(170, 240)	42.5	7.5
	(160, 70)	44.3	7.0
	(170, 60)	44.4	7.2

[a] Only conformations having energies exceeding the lowest one by less than 3 kcal mol^{-1} were considered. [b] Torsion angles corresponding to rotations of the benzophenone group of L-Bpa around the two single bonds $C^\alpha-C^\beta$ and $C^\beta-C^\gamma$ bonds connecting it to the peptide backbone. [c] The shortest distance among all the distances measured from the chromophore π-system atoms and the nitrogen atom of TOAC.

As suggested above, substantial contribution to k_3 appears to stem from the triplet lifetime τ in the L-Bpa-labeled peptides. The value reported in the literature for the free benzophenone triplet is possibly too large to apply in our conditions.[35] A reason for this reduced lifetime could be associated with intra- and intermolecular hydrogen abstraction reactions,[12] competing with triplet quenching by the radical.[38] Hydrogen abstraction could also be the factor responsible for the observed decrease of the

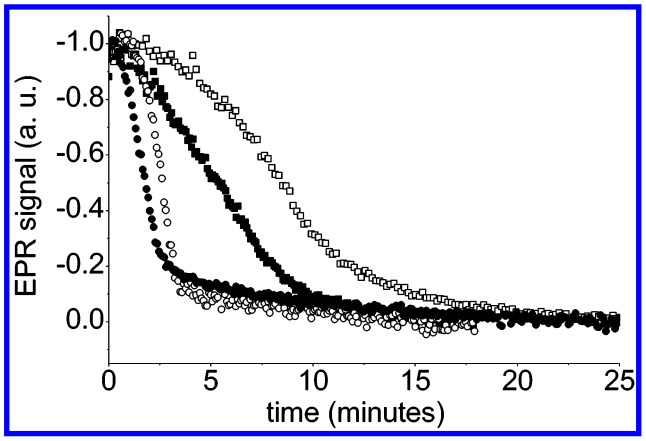

Figure 5. TR-EPR signal intensity of the central hyperfine line of the TOAC spectrum as a function of UV ($\lambda = 355$ nm) irradiation time for a 1mM solution of peptide **2**−**5** (open squares), 1 mM peptide **2**−**5** and 10 mM Boc−L−Met−OMe (open circles), 1 mM peptide **2**−**4** (full squares), 10 mM peptide **2**−**4** and 10 mM Boc−L−Met−OMe (full circles). The laser pulses had 20 Hz repetition rate. 512, 1024, or 2048 sets of 10 transient EPR signals were collected by a digital oscilloscope. Time separation between each set was about 0.5 s.

signal intensity during the TR-EPR data acquisition. This last effect is particularly pronounced for peptides **2**−**4** and **1**−**9**.

To investigate the kinetics of peptide degradation, we designed a novel experimental procedure. The magnetic field was set at the value corresponding to the central field line of the TOAC spectrum and the peptide sample was irradiated by laser pulses ($\lambda = 355$ nm). Transient EPR signals were recorded and averaged. The maximum value of the EPR transient signal was plotted as a function of irradiation time. The results indicate that degradation does occur and that it is less pronounced for peptides **2**−**3**, **2**−**5**, and **2**−**6**, compared to peptide **2**−**4**. Analogous experiments with peptide **1**−**9** showed a remarkably faster signal decay. A slower degradation is interpreted as due to the more efficient triplet quenching by TOAC in the **2**−**3**, **2**−**5,** and **2**−**6** peptides. All the investigated peptide systems degrade faster in the presence of the amino acid derivative Boc-L-Met-OMe. The Met residue is known to react quite efficiently with triplet benzophenone via hydrogen abstraction.[12] However, the above-mentioned rank order in the degradation process is maintained (i.e., TOAC seems to act as a protecting moiety against hydrogen abstraction). Figure 5 shows selected examples of the results of these experiments. However, a quantitative treatment of the experimental data is not feasible because they depend on a number of parameters, which are not fully controlled (e.g., the laser light energy absorbed by the different samples). We should also mention that, for the case of intramolecular hydrogen abstraction, the quantum yield of the degradation depends on the branching ratio of the biradical to products and back to starting materials. In principle, different peptides could have different branching ratios. We do not expect that the differences would be significant for intermolecular hydrogen abstraction.

Conclusions

The time evolution of the polarized nitroxide TR-EPR signals, obtained by irradiating a series of peptides labeled with a nitroxide radical (TOAC) and a benzophenone chromophore (L-Bpa), has been fitted by using modified Bloch equations. Their analytical solution can be approximated by a biexponential function. Under our experimental conditions, according to the proposed polarization model, the k_2 rate constant is dominated by the nitroxide relaxation time, whereas the k_3 constant is characterized by several types of contributions, including triplet quenching caused by the nitroxide, phosphorescence, and other processes, which chemically degrade the benzophenone group of L-Bpa. The intramolecular nature of the polarization process has been unambiguously demonstrated. Clearly, detection of this phenomenon is facilitated by the use of our rigid, helical peptide templates based on C^{α}-tetrasubstituted α-amino acids, which are able to keep the C^{α} atoms of the two covalently bound labels at a fixed distance. The aim of this work was to seek a parameter sensitive to the radical-triplet distance. Unfortunately, the kinetic parameters do not fulfill these requirements possibly because the side chain of one component of our dyad (L-Bpa) is rather flexible. Therefore, this chromophoric amino acid does not represent the best possible choice for an investigation of the relationship between radical-triplet distance and EPR parameters. We are currently expanding the scope of this research by exploiting a novel chromophoric, C^{α}-tetrasubstituted, helicogenic amino acid bearing a conformationally blocked side chain.

References and Notes

(1) Porter, G.; Wright, M. R. *Discuss. Faraday Soc.* **1959**, *27*, 18.

(2) (a) Hoytink, G. J. *Mol. Phys.* **1969**, *2*, 114. (b) Razi Naqvi, K.; Staerk, H.; Gillbro, T. *Chem. Phys. Lett.* **1977**, *49*, 160.

(3) Ziegler, J.; Karl, N. *Chem. Phys.* **1979**, *40*, 207.

(4) (a) Blättler, C.; Jent, F.; Paul, H. *Chem. Phys. Lett.* **1990**, *166*, 375. (b) Kawai, A.; Okutsu, T.; Obi, K. *J. Phys. Chem.* **1991**, *95*, 9130. (c) Kawai, A.; Obi, K. *J. Phys. Chem.* **1992**, *96*, 5701.

(5) (a) Shushin, A. I. *Zeit. Physik. Chem.* **1993**, *182*, 9. (b) Goudsmit, G.-H.; Paul, H.; Shushin, A. I. *J. Phys. Chem.* **1993**, *97*, 13243.

(6) de Kanter, F. J. J.; den Hollander, J. A.; Huizer, A. H.; Kaptein, R. *Mol. Phys.* **1977**, *34*, 857.

(7) Turro, N. J.; Koptyug, I. V.; van Willigen, H.; McLauchlan, K. A. *J. Magn. Reson. A* **1994**, *109*, 121.

(8) (a) Corvaja, C.; Maggini, M.; Prato, M.; Scorrano, G.; Venzin, M. *J. Am. Chem. Soc.* **1995**, *117*, 8857. (b) Corvaja, C.; Maggini, M.; Ruzzi, M.; Scorrano, G.; Toffoletti, A. *Appl. Magn. Reson.* **1997**, *12*, 477. (c) Ishi, K.; Fujisawa, J.; Ohba, Y.; Yamauchi, S. *J. Am. Chem. Soc.* **1996**, *118*, 13079. (d) Jockusch, S.; Dedola, G.; Lem, G.; Turro, N. J. *J. Phys. Chem. B* **1999**, *103*, 9126. (e) Corvaja, C.; Sartori, E.; Toffoletti, A.; Formaggio, F.; Crisma, M.; Toniolo, C.; Mazaleyrat, J.-P.; Wakselman, M. *Chem. Eur. J.* **2000**, *6*, 2775.

(9) In the case of a rigid connection, J is constant, and the time dependent perturbation responsible for quartet doublet transitions is the electron spin dipolar interaction, modulated by the molecular tumbling motion.

(10) (a) Forbes, M. D. E.; Bhagat, K. J. *J. Am. Chem. Soc.* **1993**, *115*, 3382. (b) Forbes, M. D. E.; Ruberu, S. R. J. *J. Phys. Chem.* **1993**, *97*, 13223. (c) Forbes, M. D. E. *J. Am. Chem. Soc.* **1993**, *115*, 1613. (d) Avdievich, N. I.; Forbes, M. D. E. *J. Phys. Chem.* **1995**, *99*, 9660.

(11) Toniolo, C.; Crisma, M.; Formaggio, F. *Biopolymers* (*Pept. Sci.*) **1998**, *47*, 153.

(12) Kauer, J. C.; Erickson-Viitanen, S.; Wolfe, H. R. J.; DeGrado, W. F. *J. Biol. Chem.* **1986**, *261*, 10695.

(13) Toniolo, C.; Benedetti, E. *Trends Biochem. Sci.* **1991**, *16*, 350.

(14) (a) Auvin-Guette, C.; Rebuffat, S.; Prigent, Y.; Bodo, B. *J. Am. Chem. Soc.* **1992**, *114*, 2170. (b) Toniolo, C.; Crisma, M.; Formaggio, F.; Peggion, C.; Monaco, V.; Goulard, C.; Rebuffat, S.; Bodo, B. *J. Am. Chem. Soc.*, **1996**, *118*, 4952. (c) Monaco, V.; Formaggio, F.; Crisma, M.; Toniolo, C.; Hanson, P.; Millhauser, G. L. *Biopolymers* **1999**, *50*, 239.

(15) (a) Toniolo, C.; Benedetti, E. *Macromolecules* **1991**, *24*, 4004. (b) Karle, I. L.; Balaram, P. *Biochemistry* **1990**, *29*, 6747. (c) Karle, I. L. *Acc. Chem. Res.* **1999**, *32*, 693. (d) Toniolo, C.; Crisma, M.; Formaggio, F.; Peggion, C. *Biopolymers* (*Pept. Sci.*) **2001**, *60*, 396.

(16) (a) Rassat, A.; Rey, P. *Bull. Chem. Soc. Fr.* **1967**, 815. (b) Dulog, L.; Wang, W. *Liebigs Ann. Chem.* **1992**, 301. (c) Smythe, M. L.; Nakaie, C. R.; Marshall, G. R. *J. Am. Chem. Soc.* **1995**, *117*, 10555.

(17) Carpino, L. A. *J. Am. Chem. Soc.* **1993**, *115*, 4397.

(18) (a) Jones, D. S.; Kenner, G. W.; Preston, J.; Sheppard, R. C. *J. Chem. Soc.* **1965**, 6227. (b) Benedetti, E.; Bavoso, A.; Di Blasio, B.; Pavone, V.; Pedone, C.; Crisma, M.; Bonora, G. M.; Toniolo, C. *J. Am. Chem. Soc.* **1982**, *104*, 2437.

(19) Hanson, P.; Millhauser, G.; Formaggio, F.; Crisma, M.; Toniolo, C. *J. Am. Chem. Soc.* **1996**, *118*, 7618.

(20) Moroder, L.; Hallett, A.; Wünsch, E.; Keller, O.; Wersin, G. *Hoppe Seyler's Z. Physiol. Chem.* **1976**, *357*, 1651.

(21) Hyperchem, Hypercube, Inc., Gainesville, FL.

(22) Bui, T. T. T.; Formaggio, F.; Crisma, M.; Monaco, V.; Toniolo, C.; Hussain, R.; Siligardi, G. *J. Chem. Soc., Perkin Trans.* **2000**, *2*, 1043.

(23) (a) Mizushima, S.; Shimanouchi, T.; Tsuboi, M.; Souda, R. *J. Am. Chem. Soc.* **1952**, *74*, 270. (b) Palumbo, M.; Da Rin, S.; Bonora, G. M.; Toniolo, C. *Makromol. Chem.* **1976**, *177*, 1477.

(24) Toniolo, C.; Bonora, G. M.; Barone, V.; Bavoso, A.; Benedetti, E.; Di Blasio, B.; Grimaldi, P.; Lelj, F.; Pavone, V.; Pedone, C. *Macromolecules* **1985**, *18*, 895.

(25) Kennedy, D. F.; Crisma, M.; Toniolo, C.; Chapman, D. *Biochemistry* **1991**, *30*, 6541.

(26) Toniolo, C.; Peggion, C.; Crisma, M.; Formaggio, F.; Shui, X.; Eggleston, D. S. *Nature: Struct. Biol.* **1994**, *1*, 908.

(27) (a) Crisma, M.; Monaco, V.; Formaggio, F.; Toniolo, C.; George, C.; Flippen-Anderson, J. L. *Lett. Pept. Sci.* **1997**, *4*, 213. (b) Monaco, V.; Formaggio, F.; Crisma, M.; Toniolo, C.; Hanson, P.; Millhauser, G.; George, C.; Deschamps, J. R.; Flippen-Anderson, J. L. *Bioorg. Med. Chem.* **1999**, *7*, 119.

(28) Goudsmith, G. H.; Paul, H. *Chem. Phys. Lett.* **1993**, *208*, 73.

(29) (a) Percival, P. W.; Hyde, J. S. *J. Magn. Reson.* **1976**, *23*, 249. (b) Hwang, J. S.; Mason, R. P.; Hwang, L. P.; Freed, J. H. *J. Phys. Chem.* **1975**, *79*, 489.

(30) The response rate of our experimental apparatus ($\sim 6.5 \times 10^6$ s^{-1}) is high enough not to appreciably influence the measured rate constants.

(31) Corvaja, C.; Sartori, E.; Toffoletti, A.; Formaggio, F.; Crisma, M.; Toniolo, C. *Biopolymers* **2000**, *55*, 486.

(32) Heisenberg spin exchange operates in the following way. When two free radicals having different electron spin *z* components (α and β) encounter each other, they could exchange their spins. If these radicals are characterized by different nuclear spin components (e.g. M_I for the α one and M_I' for the β one) the exchange process corresponds to transfer the electron α spin on the radical with the different nuclear component, that is, M_I'. The same phenomenon occurs for the β spin that is transferred to the radical with nuclear component M_I. Therefore, Heisenberg spin exchange produces a polarization (excess of α or β spins) distribution among the different nuclear spin components. For nitroxides (^{14}N spin I = 1), the $M_I = 0$ hyperfine component is not affected, because the corresponding polarization has equal chance of being increased or decreased by collisions of $M_I = 0$ radicals with those with $M_I = 1$ and those with $M_I = -1$.

(33) The triplet benzophenone decay time in acetonitrile at room temperature is 50 μs (Wallace, W. L.; Van Duyne, R. P.; Lewis, F. D. *J. Am. Chem. Soc.* **1976**, *98*, 5319).

(34) Kobori, Y.; Takeda, K.; Tsuji, K.; Kawai, A.; Obi, K. *J. Phys. Chem. A* **1998**, *102*, 5160.

(35) 373 cP at 290 K (Yaws, C. L. In *Handbook of Viscosity*; Gulf Publishing Company: Houston, TX, 1995; Vol. 1, p 327).

(36) The spectrum of the 1 mM **5** and benzophenone mixture was not used for the simulations and the kinetic discussion because of its very low signal-to-noise ratio ($\sim$2).

(37) Only the minimum energy conformations separated from the lowest one by no more than 3 kcal mol^{-1} were chosen for distance calculations.

(38) An additional proof came from experiments carried out on a mixture of peptides **1** and **5**. As in this case only an intermolecular quenching process could be operative, the quenching rate constant should be even smaller than for the **5** + **B** case, because the steric bulkiness of peptide **1** is significantly larger than that of benzophenone. Indeed, such a mixture gave a value of $k_3 = 0.34 \times 10^6$ s^{-1} when both peptides were 1 mM, smaller than in all other cases. However, this value was $k_3 = 0.72 \times 10^6$ s^{-1} when both peptides were 5 mM, thus showing a concentration dependence stronger than in all other cases. An intermolecular hydrogen abstraction could explain this behaviour.